JOURNAL OF COMPUTATIONAL PHYSICS 88, 284–304 (1990)

A Mixed Finite Element Formulation for Maxwell's Equations in the Time Domain

ROBERT L. LEE AND NIEL K. MADSEN

Lawrence Livermore National Laboratory,
University of California, Livermore, California 94550

Received September 2, 1988; revised July 14, 1989

A Galerkin finite element solution technique for the Maxwell's equations is discussed. This new formulation can be viewed as a generalization of certain staggered-grid finite difference schemes to arbitrary meshes. It is shown that this technique is simple to implement and is more accurate as well as more cost effective than the standard equal-order finite element approach. Numerical are presented to evaluate the performance of this new element relative to the standard element. © 1990 Academic Press, Inc.

1. INTRODUCTION

The classical approach to solve the linear Maxwell's equations in free space is to use Fourier transform methods. Many useful analytical solutions have been obtained via this approach. However, when the domain of interest involve irregularly-shaped boundaries or is finite in extent or when variable dielectric properties are considered, analytic solutions can no longer be obtained and numerical approaches must be employed. Over the past two decades, finite difference techniques have been used extensively to generate approximate solutions to the Maxwell's equations. While it is well known that the finite difference approach can produce accurate results on rectangular or almost rectangular domains, there is difficulty in extending this approach to more general domains. Here the typical techniques used are to either employ a "stair-stepped" approximation to the irregular boundary or to invoke a global (usually numerical) transformation wherein the original domain is mapped into a rectangle in the transformed coordinates. The former technique is clearly a rather poor approximation to the boundary shape unless a very fine resolution of grid points is used and the latter results in a more complicated set of equations to be solved.

The Galerkin finite element technique has been widely used to solve problems associated with irregularly-shaped domains in many engineering problems. One of the first applications of finite elements to electromagnetic problems was by Arlett *et al.* [1] who used this technique to calculate the modal shape of a field for a wave guide problem. Over the past decade, many papers and several books have been written concerning the use of this approach to the boundary value problems in con-

0021-9991/90 $3.00

junction with electrostatics [2, 3]. It is clear that finite elements have already been well established in the solution of steady-state electromagnetic problems. However, the extension of this technique to time domain problems has not been very extensive. Lynch *et al.* [4] have developed a finite element model based on a second-order wave equation to solve electromagnetic problems in the frequency domain. More recently, Cangellaris *et al.* [5] have developed a collocation method in conjunction with a conforming mesh for the time-domain computation of electromagnetic scattering problems. To date, most of the publications in the area of time-domain solutions of Maxwell's equations have been based on finite difference rather than finite element techniques [6, 7].

In this paper, we will present a mixed Galerkin finite element formulation of the Maxwell's equations in the time domain. For convenience we will discuss details of the formulation only for two dimensions, however the algorithms suggested can be generalized to three dimensions in a straightforward manner. The Galerkin elements integrals are computed analytically and an explicit forward–backward time-integration scheme is employed for advancing the resulting set of ordinary differential equations in time. We will discuss the relative merits of three simple finite element approximations to the field variables all of which are based on variants of 4-node bilinear elements. These are: (1) An equal-order interpolation element in which both the electric field (E_x and E_y) and the magnetic field (H_z) are approximated by bilinear basis functions; (2) a mixed-interpolation element in which the electric field is approximated bilinearly and the magnetic field as piecewise constants; and (3) a mixed-interpolation element in which the electric field is approximated as piecewise constants and the magnetic field as bilinear functions. The latter two approximations may be viewed as finite element analogs to certain staggered-grid finite difference schemes. Several numerical examples will be presented to evaluate the accuracy of two of these three elements.

We will also discuss the generalization of this model to solve problems involving material interfaces with different dielectric properties. Numerical examples will be presented and compared with analytical solutions.

2. Governing Equations

We are interested in solving the equations associated with the scattering of electromagnetic waves from arbitrarily-shaped objects. For simplicity we will focus attention on wave propagation within linear isotropic media. The relevant equations are given by the Maxwell's equations written in the form:

$$\varepsilon \frac{\partial \mathbf{E}}{\partial t} = \nabla \times \mathbf{H} - \mathbf{J}, \tag{1}$$

$$\mu \frac{\partial \mathbf{H}}{\partial t} = -\nabla \times \mathbf{E}. \tag{2}$$

where, in two dimensions, the electric (**E**) and magnetic (**H**) field vectors are $(E_x, E_y, 0)$ and $(0, 0, H_z)$, respectively. The material properties of the medium are the permitivity ε, the permeability μ and the conduction current current density is represented by **J**. For generality, material properties are permitted to be spatially varying.

The Eqs. (1) and (2) are solved within an irregular domain Ω enclosed by boundary Γ. In order to render the problem well-posed, appropriate external boundary conditions must be chosen. Generally, for a closed domain it is sufficient that the tangential component of the electric vector (E_t) is prescribed along Γ. In the case of metallic surfaces E_t is simply set equal to zero. For open domains more complicated "free-space" conditions must be developed at the computational boundaries. Generally special treatment is also required at material interfaces. The details of this procedure will be discussed later in a separate section.

3. The Finite Element Formulation

The finite element discretization of Eqs. (1) and (2) is performed via the conventional Galerkin method. We assume the electrical and magnetic fields are approximated by:

$$\mathbf{E}^h = \sum_{i=1}^{N_E} \mathbf{E}_i(t)\, \phi_i(\mathbf{x})$$

and

$$\mathbf{H}^h = \sum_{i=1}^{N_H} \mathbf{H}_i(t)\, \psi_i(\mathbf{x}), \tag{3}$$

where there are N_E nodes for the electric field vector and N_H nodes for the magnetic field. When the basis functions ϕ_i and ψ_i are piecewise polynomials of the same order, the interpolations are known as equal-order and is referred to in this paper as the "linear E," "linear H," or ELHL formulation. In contrast, if the basis functions are of different order (typically one of the sets being one order lower than the other), the approximations are termed to be mixed interpolations. We suggest that these mixed-interpolation representations may be viewed as generalizations of staggered-grid discretization schemes to distorted meshes wherein one of the fields is defined at the nodal points while the other field is defined at the element centroids. The first application of mixed-interpolation finite element schemes to hyperbolic equations appears to be due to Williams and Zienkiewicz [8] who considered the one-dimensional shallow water equations.

In this paper we focus attention on one of the simplest two-dimensional mixed-interpolation approximation which is given by piecewise-continuous (C°) bilinear functions for H in conjunction with (discontinuous) piecewise-constant functions for E, henceforth referred to as the "constant E," "linear H," or ECHL formulation.

Other combinations are obviously possible, such as those obtained by interchanging the approximations for E and H (referred to as the "linear E," "constant H," or ELHC formulation) and will also be discussed. We note that yet another class of linear elements can be developed by employing basis functions which vary linearly in one direction and are constant in the remaining direction within each element. This approximation leads to a scheme in which the variables are staggered and defined on the midsides of the element [9]. Because of its excellent phase properties, many finite difference electromagnetic models employ this particular arrangement of variables on rectangular meshes. As a result of some recent work [10], this pattern of staggering has been shown to perform well on distorted meshes when a modified finite volume technique is used. For nonrectangular meshes containing many distorted elements, the finite volume approach appears to be more complicated and concomitantly more expensive than the approach suggested here. In this paper we will limit our discussions to the equal-order ELHL element and the ECHL and ELHC mixed-interpolation elements.

Following the Galerkin procedure, a system of discretised equations can be obtained by premultiplying Eqs. (1) and (2) with an appropriate set of basis functions and integrating over the domain Ω, giving

$$\int_\Omega \varepsilon\phi_i \frac{\partial \mathbf{E}}{\partial t} = \int_\Omega \phi_i \nabla \times \mathbf{H} - \int_\Omega \phi_i \mathbf{J}; \qquad i = 1, ..., N_E, \tag{4}$$

$$\int_\Omega \mu\psi_i \frac{\partial \mathbf{H}}{\partial t} = -\int_\Omega \psi_i \nabla \times \mathbf{E}; \qquad i = 1, ..., N_H. \tag{5}$$

When either E or H is approximated as piecewise constant functions, it is necessary to invoke Stokes' theorem (or integration-by-parts) to the appropriate terms on the right-hand side of Eq. (4) or (5). This procedure leads to the "weak" form of the equations, which, for the ECHL formulation is given by

$$\int_\Omega \mu\psi_i \frac{\partial \mathbf{H}}{\partial t} = -\oint_\Gamma (\mathbf{n} \times \mathbf{E})\, \psi_i + \int_\Omega \nabla\psi_i \times \mathbf{E} \tag{6}$$

and for the ELHC formulation by

$$\int_\Omega \varepsilon\phi_i \frac{\partial \mathbf{E}}{\partial t} = \oint_\Gamma (\mathbf{n} \times \mathbf{H})\phi_i - \int_\Omega \nabla\phi_i \times \mathbf{H} - \int_\Omega \phi_i \mathbf{J}. \tag{7}$$

In the boundary terms on the right-hand side of Eqs. (6) and (7), $\mathbf{n}$ is the outer normal unit vector and the resulting integrals are referred to as "natural" boundary conditions. These boundary conditions may be implemented by evaluating the boundary integrals. The boundary term for the ECHL formulation can be easily evaluated since $\mathbf{n} \times \mathbf{E}$ is identically E_t and is typically specified as boundary condition. When the boundary is a perfect conductor, $E_t = 0$, and, therefore, the integral in Eq. (6) simply vanishes. In contrast, the boundary term associated with the

ELHC formulation which involves $\mathbf{n}\times\mathbf{H}$ or H_t is an unknown quantity; thus the integral cannot be evaluated directly. For the case in which E_t is specified at the boundary, the corresponding nodal equation is omitted (being replaced by its specified value) and the integral term involving $\mathbf{n}\times\mathbf{H}$ does not need to be evaluated. This procedure of omitting the nodal equation and replacing the corresponding unknown with its specified value is used for all "essential" or specified boundary conditions. It is noteworthy that, with both the ELHC and ELHL formulations, E_t can be imposed directly at the boundary nodes (as essential conditions) whereas in the case of the ECHL formulation E_t can be satisfied only in a "weak" sense via the source term of Eq. (6). This is entirely consistent with the element-based approximation of E in the ECHL formulation which contrasts with the nodal-based approximations of the alternative formulations.

Upon substituting the approximate solutions E and H into the appropriate sets of Eqs. (4) to (7) and assuming that the current density J can be interpolated as a sum of the ϕ_i's, the spatially discretized form of the partial differential equations in two dimensions are given symbolically by

$$A_\varepsilon \dot{u} = Bu + AJ + F, \tag{8}$$

where the vector of nodal unknown u denotes (E_x, E_y, H_z), with $\dot{u}$ being its time derivative, and J is the nodal analog of $(J_x, J_y, 0)$. The submatrices of A_ε, A, B, and F can be expressed in terms of the Galerkin integrals by defining:

$$\begin{aligned}
M_\varepsilon &= \int_\Omega \varepsilon \Phi \Phi^{\mathrm{T}}, & M_E &= \int_\Omega \Phi \Phi^{\mathrm{T}}, \\
M_\mu &= \int_\Omega \mu \Psi \Psi^{\mathrm{T}}, & M_H &= \int_\Omega \Psi \Psi^{\mathrm{T}}, \\
C_x &= \int_\Omega \Phi \frac{\partial \Psi^{\mathrm{T}}}{\partial x}, & C_y &= \int_\Omega \Phi \frac{\partial \Psi^{\mathrm{T}}}{\partial y}, \\
D_x &= \int_\Omega \frac{\partial \Psi}{\partial x} \Phi^{\mathrm{T}}, & D_y &= \int_\Omega \frac{\partial \Psi}{\partial y} \Phi^{\mathrm{T}},
\end{aligned} \tag{9}$$

with the superscript "T" denoting the transpose of a matrix. Using the above integral representations, the mass matrices A_ε and A can be written as

$$A_\varepsilon = \begin{bmatrix} M_\varepsilon & 0 & 0 \\ 0 & M_\varepsilon & 0 \\ 0 & 0 & M_\mu \end{bmatrix}, \qquad A = \begin{bmatrix} M_E & 0 & 0 \\ 0 & M_E & 0 \\ 0 & 0 & M_H \end{bmatrix}. \tag{10a}$$

The form of the matrices B and F depend on the approximations employed and are given (prior to imposition of essential boundary conditions) for the ELHL formulation by

$$B=\begin{bmatrix} 0 & 0 & C_y \\ 0 & 0 & -C_x \\ D_y & -D_x & 0 \end{bmatrix}, \qquad F=\begin{bmatrix} 0 \\ 0 \\ 0 \end{bmatrix}, \tag{10b}$$

and for the ELHC formulation by

$$B=\begin{bmatrix} 0 & 0 & -D_y^T \\ 0 & 0 & D_x^T \\ D_y & -D_x & 0 \end{bmatrix}, \qquad F=\begin{bmatrix} \oint_\Gamma n_y H_z \phi_i \\ -\oint n_x H_z \phi_i \\ 0 \end{bmatrix}, \tag{10c}$$

and lastly for the ECHL formulation by

$$B=\begin{bmatrix} 0 & 0 & C_y \\ 0 & 0 & -C_x \\ -C_y^T & C_x^T & 0 \end{bmatrix}, \qquad F=\begin{bmatrix} 0 \\ 0 \\ \oint_\Gamma (E_x n_y - E_y n_x)\psi_i \end{bmatrix}. \tag{10d}$$

We note that nonhomogeneous material properties can be easily incorporated by assuming a piecewise constant variation over each element and assembling "material-weighted" element mass matrices M_ε and M_μ, e.g., $M_\varepsilon = \Sigma_e \varepsilon^e M_\varepsilon^e$.

In the finite element approximation, bilinear elements are represented by 4-noded, straight-sided quadralaterals. The basis functions associated with the elements are given in standard texts such as Zienkiewicz [11] and will not be repeated here. In order to compute the element matrices of Eqs. (10), the finite element integrals are usually transformed into local coordinates via isoparametric mapping and evaluated by Gaussian quadrature techniques. Our early attempts in using very efficient, but approximate, one-point quadratures to evaluate the Galerkin integrals failed due to problems with temporal instabilities. However, because the particular terms of Eq. (9) involve only products of polynomials, element integrals can be obtained *exactly* as analytic functions of the nodal coordinates [12]. With this procedure element-level matrices can be easily calculated, on the fly, and the usual requirement of storing these matrices in memory (or on peripheral disks) can be avoided. This computational strategy is especially important for three-dimensional problems where the in-core memory of even the largest machines can often be exceeded.

4. Time-Integration Scheme

Various time-integration schemes can be used to advance the solutions to Eq. (8) in time. For efficiency reasons we chose to employ an explicit time-integration scheme rather than a more robust, but expensive, implicit scheme. Although it is well known that implicit schemes are not subjected to timestep limitations as exhibited by explicit schemes, the tracking of propagating wave fronts require rather small timesteps in order to maintain good phase accuracy. Because of this restriction it appears that the computationally simpler explicit schemes are more

suitable for this class of problems. Perhaps the most widely used explicit time-integration scheme is the three-time level, second-order accurate, leap-frog scheme. In this model we employ a variant of the leap-frog scheme which is based on a forward–backward procedure. The timestep procedure applied to, for example, the ECHL equations are given by

$$E_x^{n+1} = E_x^n + M_\varepsilon^{-1}(C_y H_z^n - M_E J_x^n)\,\Delta t, \tag{11a}$$

$$E_y^{n+1} = E_y^n + M_\varepsilon^{-1}(-C_x H_z^n - M_E J_y^n)\,\Delta t, \tag{11b}$$

$$H_z^{n+1} = H_z^n + M_\mu^{-1}(-C_y^T E_x^{n+1} + C_x^T E_y^{n+1} + F^n)\,\Delta t. \tag{11c}$$

In the above equations, (11a) and (11b) are forward-Euler steps for E while Eq. (11c) is a backward-Euler step for H_z. A similar scheme has been used in the integration of the shallow water equations [13].

It is well known that consistent mass matrices present a major difficulty in the efficient implementation of explicit schemes. When bilinear basis functions are used, M are banded sparse matrices and their inverses M^{-1} are dense matrices which must be stored. In order to avoid this problem, Donea [14] developed an iterative method which approximate the effect of the consistent mass matrix without incurring the cost of a full matrix inversion. This procedure is based on the lumped mass matrix M_L with the solution at each time step $n+1$ obtained iteratively via the following steps:

$$\begin{aligned} &M_L u_{(0)}^{n+1} = f^n, \\ &M_L u_{(i+1)}^{n+1} = f^n - (M - M_L) u_{(i)}^{n+1}, \qquad \text{for} \quad i \geqslant 0 \end{aligned} \tag{12}$$

where

$$M_L = \int_\Omega \Phi,$$

and "i" is the iteration number. In Eq. (12), the computation of M^{-1} is trivial since it is diagonal. Two or three iterations per timestep are usually sufficient to yield good accuracy for most problems.

While the full treatment of consistent mass matrix is desirable for achieving superior phase speed properties (see, for example, Fig. 1), many explicit time integration algorithms employ the significantly simpler, but less accurate, lumped mass approximation and compensate somewhat by using a finer mesh to permit higher resolution of the waves. This appears to be a reasonable approach especially for equal-order formulation where M^{-1} appears in the equations for each variable (see Eq. (11)). It is noteworthy, however, that if mixed-interpolation is used and ϕ_i is chosen to be piecewise-constant, the mass matrix in Eqs. (11a) and (11b) is identically diagonal. Thus computation with the fixed-formulation is distinctly simpler than for the equal-order formulation. Moreover, the dimensions of the C and D matrices in Eqs. (10c) and (10d) are somewhat smaller for the mixed case thus less computational effort is required to generate the right-hand side vectors of Eq. (11).

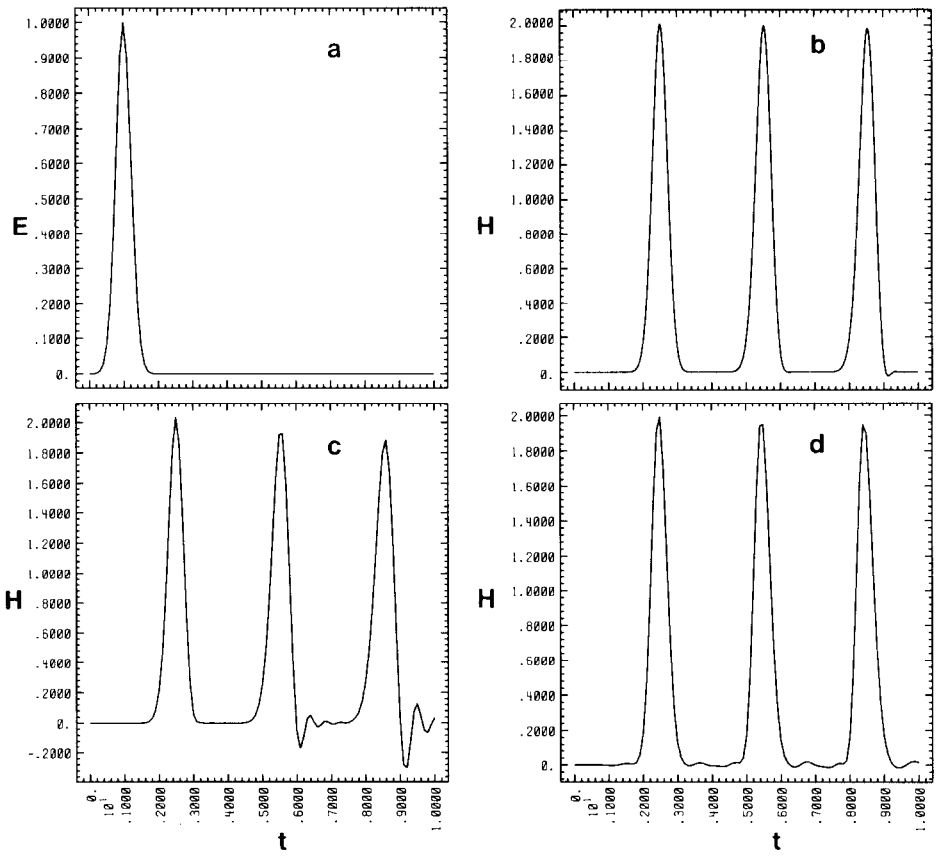

FIG. 1. Propogation of Gaussian waveform in one dimension: (a) prescribed E at the left boundary; time histories of H at the right boundary; (b) ECHL solution; (c) ELHL lumped mass solution; (d) ELHL consistent mass solution.

5. Treatment of Curved Boundaries and Material Interfaces

Finite element formulations typically employ a cartesian coordinate system with the unknown degrees of freedom given by the cartesian components of the vector field variables. In such a coordinate system, the constrained degrees of freedom (which are usually associated with prescribed boundary conditions) can be easily treated when boundary surfaces are aligned with the coordinate directions. If the boundary shapes are irregular, the usual algorithms for incorporating normal and tangential boundary constraints for cartesian coordinate systems are no longer applicable. Furthermore, it is evident that there is difficulty in uniquely defining the normal direction at a node which is formed by two piecewise continuous line segments. For the electromagnetic problems considered here, improper choice of

the normal directions may lead to a numerical scheme which does not satisfy the relevant conservation laws.

Engleman *et al.* [15] developed an algorithm for determining a consistent normal by invoking arguments associated with the conservation of mass in incompressible flows. Following their reasoning one can obtain identical formulae by invoking the requirement of conservation of charge. Our implementation of the boundary algorithm follows closely with that of Engelman in which the consistent normal at node "i" is given by

$$n_{x_i} = \frac{1}{n_i} \int_\Omega \frac{\partial \phi_i}{\partial x} \, d\Omega,$$
$$n_{y_i} = \frac{1}{n_i} \int_\Omega \frac{\partial \phi_i}{\partial y} \, d\Omega, \tag{13}$$

where $n_i = [\int (\partial \phi_i/\partial x)^2 + \int (\partial \phi_i/\partial y)^2]^{1/2}$ and ϕ_i is the ith nodal basis function. The projections n_{x_i} and n_{y_i} at a node can be written analytically in terms of the coordinates of its nearest neighbours in the form

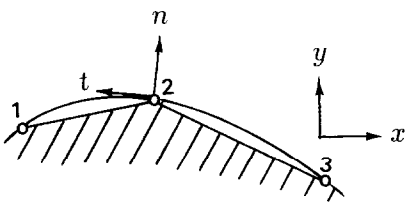

$$n_{x_2} = \frac{y_1 - y_3}{[(x_1 - x_3)^2 + (y_1 - y_3)^2]^{1/2}},$$
$$n_{y_2} = \frac{x_3 - x_1}{[(x_1 - x_3)^2 + (y_1 - y_3)^2]^{1/2}}. \tag{14}$$

Once the nodal normals are determined, the nodal equations at the boundary are locally rotated to the normal and tangential directions. The original variables (E_x and E_y) are then transformed into E_n and E_t and the constraints are applied directly to these unknowns. This procedure has an important advantage in that the modifications of the nodal coefficients for the rotated variables can be performed entirely at the element level. Upon assembly of the global matrix the constraint degrees of freedom for the normal and tangential nodal components can be imposed in the usual manner as for the unrotated system.

It is well known that the appropriate conditions at the interface of two adjoining media with different material properties is given by

$$\mathbf{n} \cdot (\mathbf{D}_2 - \mathbf{D}_1) = \rho_s; \qquad \mathbf{n} \times (\mathbf{E}_1 - \mathbf{E}_2) = 0;$$
$$\mathbf{n} \cdot (\mathbf{B}_2 - \mathbf{B}_1) = 0; \qquad \mathbf{n} \times (\mathbf{H}_2 - \mathbf{H}_1) = J_s, \tag{15}$$

where D, B, ρ_s, and J_s are the displacement vector, the magnetic induction vector, the surface charge density and the surface current density at the interface, respectively. In the simplest setting, we assume ρ_s and J_s are zero, and the constitutive equations are given by $D = \varepsilon E$ and $B = \mu H$.

For materials in which typically only the dielectric constant change across an interface, the normal component of the electric field (E_n) is discontinuous across the interface and it is required that

$$\varepsilon_1(\mathbf{n} \cdot \mathbf{E})_1 = \varepsilon_2(\mathbf{n} \cdot \mathbf{E})_2 \tag{16}$$

with ε_1 and ε_2 being the dielectric constants of the two materials. We note that if the E fields are calculated at the nodes (as for the ELHL or ELHC formulations), the constraint of Eq. (16) must be imposed at all interfaces nodes. In principle if Eq. (16) is not satisfied the conservation of surface charge may be violated. The implementation of such an interface constraint into a numerical model can be accomplished by observing that the displacement vector (D) *is* continuous across the interface. Rather than computing E_n and E_t at interface nodes it is straightforward to, instead, employ as variables D_n and E_t, both of which are continuous. Upon calculation of D_n, the corresponding values of E_n on either side of the interface can be obtained by invoking the constitutive equations.

It is important to note that interfacial discontinuities involving changes in dielectric constants are automatically incorporated, albeit in a "weak" sense, into the ECHL formulation since the E nodes are never located at interfaces. Thus, in contrast to the ELHC or ELHL formulations, constraints conditions such as given by Eq. (16) do not have to specifically imposed.

6. Computational Considerations

From a computational viewpoint, the cost per timestep of the ELHL formulation is higher than that of either mixed (ECHL or ELHC) formulations for two-dimensional problems. In addition, an important simplification of the consistent mass matrix results when piecewise-constant basis functions are employed since the matrix is then diagonal. With the proposed explicit time integration procedure, the ECHL formulation (with all but one of the mass matrices being diagonal) is computationally cheaper than the ELHC formulation and, furthermore, is significantly cheaper than the ELHL formulation (where none of the mass matrices are diagonal). It is noted that this advantage in efficiency of the ECHL over the ELHC formulation does not carry over to three dimensions since both forms display the same number of diagonal and nondiagonal mass matrices. However, if lumped mass approximations are used for all of the mass matrices, the computational efficiencies of the three formulations are roughly similar, with the mixed interpolation cases being slightly cheaper due to the smaller dimension of the matrices.

The element-based definition of E for ECHL has also several distinct advantages

over the nodal based E formulations which we will now summarize. We noted earlier that material interface conditions are automatically incorporated in a weak sense into ECHL. Furthermore, when nonzero values of E_t are prescribed along curved boundaries, the boundary conditions can be easily imposed via boundary integrals of E_t (see Eq. (6)) rather than requiring local rotations of boundary nodes to normal and tangential coordinates as in the case of the ELHC and ELHL formulations. Finally, any nodal singularities of E (e.g., at corners or the origin for axisymmetric problems) are avoided since these cannot coincide with the E unknowns for the ECHL formulation which are defined at the element centroids.

Apart from boundary condition considerations, the lumped mass approximations for the ECHL and the ELHC formulations generate the same spatially discretized form of the equations on rectangular grids. Therefore the two formulations, in principle, exhibit the same phase accuracy, Although the results have not been presented, we have observed numerically that the ECHL and ELHC solutions also display approximately the same order of accuracy on distorted finite element meshes [10]. In terms of implementation, however, the ECHL formulation is generally simpler than the ELHC formulation and is therefore preferred. For this reason, the numerical results presented will focus attention on comparing the accuracy of the ELHL and ECHL formulations only.

7. Numerical Examples

Three numerical examples are considered to compare the performance of the ECHL and ELHC approximations. In order to minimize the various combinations of consistent versus lumped matrix formulations which can be tested, we have chosen to employ, for the ECHL element, mass lumping on the H_z equation while (diagonal) consistent mass matrices are used in conjunction with the E equations. Thus no iteration of the mass matrix is required for the mixed formulation. In contrast, we used either consistent or lumped mass for all of the equations associated with the ELHL formulation. For convenience as well as for graphical purposes, all element-centered quantities are extrapolated to the nodes via an area-weighted averaging procedure [16] given by

$$E_i = \frac{\sum_{j=1}^{m} S_j E_j^e}{\sum_{j=1}^{m} S_j},$$

where S_j and E_j^e are the elemental areas and values, respectively, and the summation is performed over the "m" elements which share node "i."

We begin by performing calculations on the propagation of a Gaussian-like wave form within a one-dimensional domain enclosed by perfect-conducting metal boundaries. Next we consider the two-dimensional problem of scattering of a plane wave from a cylinder in free space. In our final example, we present results from a calculation involving the propagation and scattering of a plane wave on a circular

interface separating media with different dielectric constants. For simplicity all current sources and surface charges are assumed to be zero in the example problems.

7.1. *Propagation of a Wave in One Dimension*

We first consider a one-dimensional problem involving the propagation of a finite amplitude wave within a uniform mesh. For convenience ε and μ are chosen to be unity. A Gaussian-like pulse (Fig. 1a) is introduced into the domain by prescribing a time-varying electric field at the left boundary and is given by

$$E(t) = \begin{cases} \{\exp[-10(t-1)^2] - \exp(-10)\}/\{1-\exp(-10)\}; & 0 \geqslant t \geqslant 2, \\ 0; & t > 2. \end{cases}$$

At the right boundary we impose a metal (E = 0) boundary condition thus permitting reflections to occur. A uniform mesh of 30 elements with $\Delta x = 0.05$ is used. The integrations are performed with a timestep of 0.01 resulting in Courant number of 0.2. The time variation of the magnetic field at the right boundary node is displayed in Fig. 1 for the ECHL, ELHL lumped mass and the ELHL consistent mass formulations. We note that the spatial discretization of the lumped mass ELHL formulation is identical to that of the form given by standard centered finite difference.

The results clearly show that the ECHL approximation exhibits significantly higher phase accuracy (for the high wave number components of the spectrum in particular) than the ELHL approximation and is indistinguishable from the exact solution. The ECHL solution is, in fact, more accurate than the consistent mass ELHL solution in which some wiggles are evident. It is noteworthy that in order to achieve an accuracy displayed by the ECHL solution, the ELHL calculation must be performed on a mesh which contains twice as many grid points. This is consistent with one-dimensional truncation error analysis which show that, on an uniform mesh, staggered schemes typically exhibit an accuracy which is similiar to that of an unstaggered scheme with approximately twice the grid resolution.

7.2. *Scattering of a Plane Wave on a Circular Cylinder*

The scattering of a plane electromagnetic wave from a circular cylinder in free space is one of the few nontrivial two-dimensional problems in which an analytical solution is given [17]. For these calculations we assume a rightward-propagating incident wave with a waveform identical to that shown in Fig. 1a but with an amplitude of $\sqrt{\mu_0/\varepsilon_0}$ and time scaled in nanoseconds (ns = 10^{-9} s). MKS units are used in this and in the subsequent calculation with the free space values of $\varepsilon_0 = 8.85 \times 10^{-12}$ F/m^2 and $\mu_0 = 1.2566 \times 10^{-6}$ N/A^2. The effect of the plane wave is simulated by computing analytically the associated tangential component of the electric field at the surface of the cylinder and imposing that as the boundary condition. The computational domain (only half of which is computed due to symmetry) consists of a uniform radial mesh of 15 by 30 elements and is shown in Fig. 2. We used the following boundary conditions for the problem: (i) $E_t = 0$ at $r = 1.1$;

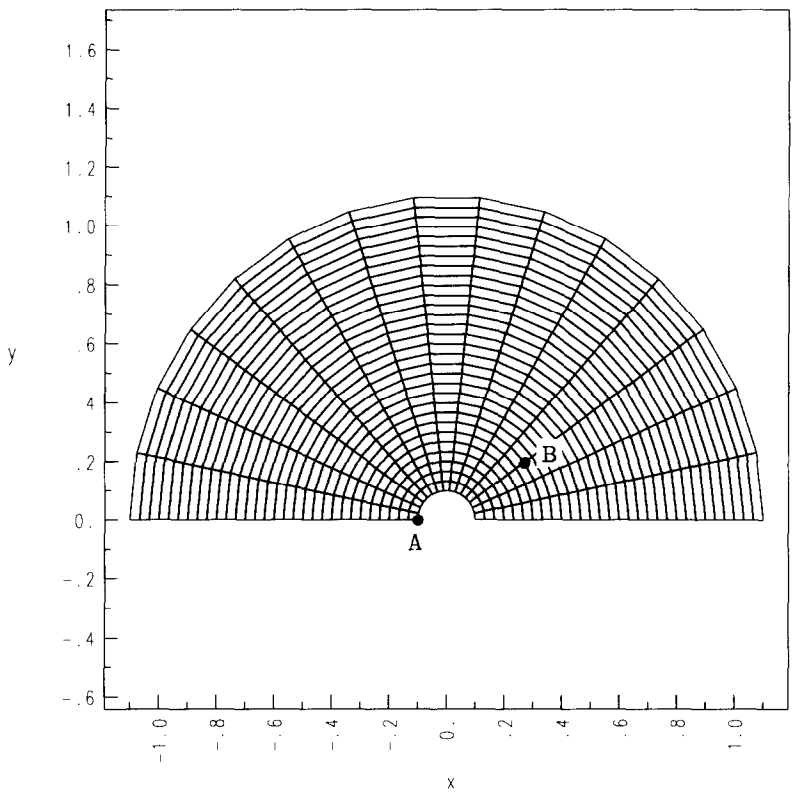

FIG. 2. The computational mesh for the problem of wave-scattering over a circular cylinder with the locations of the observation points.

(ii) $E_x = 0$ at $y = 0$ (symmetry condition); and, (iii) on the cylinder ($r = 0.1$) the Gaussian pulse is modelled by prescribing $E_t = -\sqrt{\mu_0/\varepsilon_0}\{\exp(-10\zeta^2) - \exp(-10)\} \cos\theta/\{1 - \exp(-10)\}$, where $\zeta = \{t - (x - 0.1)\sqrt{\varepsilon_0\mu_0}\}\ 10^9 - 1$ and θ is the angle measured from the positive x-axis. In order to minimize the influence of the computational boundaries we have chosen to compute the scattered (i.e., total minus incident) fields over a period of time in which the solution has not been contaminated by reflections. Integration is performed up to a time of 5 ns with a timestep of 0.05 ns.

We present in Fig. 3 the calculated time histories of the magnetic field at nodes A and B. Also shown are the exact solutions at these nodes. It is evident that the ECHL solution is significantly more accurate than the ELHL lumped mass solution. As for the earlier one-dimensional results, the ECHL solution display a much smoother result than the lumped mass ELHL solution in which wiggles are present. The consistent mass results (not presented) exhibit an accuracy somewhat closer to the ECHL solution but with observably larger oscillations. Further calculations have shown that the ECHL accuracy is approximately equal to that of ELHL for

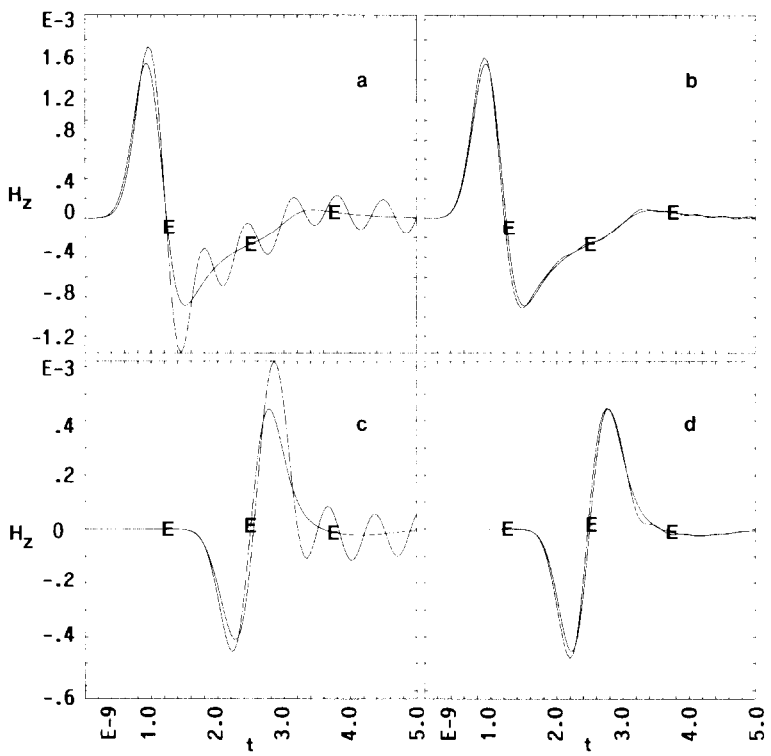

FIG. 3. Computed versus exact (E) time history solutions for the cylinder scattering problem at the observation points in Fig. 2; node A: (a) lumped mass ELHL; (b) ECHL; node B: (c) lumped mass ELHL; (d) ECHL.

a mesh with quadruple the number of elements in the present mesh. In spite of the two-dimensional character of this problem, the results appear to be consistent with those obtained for the one-dimensional solutions.

7.3. *Propagation of a Plane Wave across a Cylindrical Material Interface*

When a plane wave impinges upon on interface in which material properties change, a portion of the incident wave is reflected while the remainder is transmitted through the new medium. Exact solutions are available for simple one-dimensional problems where a material interface separates two infinite media with uniform properties. In higher dimensions, however, numerical approaches are usually required. We consider here a two-dimensional problem in which a finite amplitude wave propagating within free space is launched at a cylinder with a dielectric constant which is different than the original medium. The wave is then transmitted through the cylinder finally emerging at the opposite end after undergoing internal reflections within the circular material interface. An analytical solution can be obtained for this particular problem [17] and is used as the reference for assessing the accuracy of the numerical solutions.

The computational domain of interest, shown in Fig. 4, consists of a semi-circular section with radius 0.25 m which is imbedded within a larger rectangular region. The finite element mesh (which represents half of the full domain due to symmetry) contains 992 elements and 1059 nodes. We assume that the dielectric constant within the circular domain has a uniform value of $\varepsilon_0/16$ which contrasts with the free space value of ε_0 outside of the cylinder. The permeability μ_0 is uniform within the entire domain. We note that the speed of the waves within the material cylinder is quadruple that of the incident medium. This unusual (and somewhat artificial)

nal computational boundaries. The numerical results will, of course, be relevant only up to a time when the spurious reflections appear. It is noted that the large difference in the magnitude of the dielectric constants should tend to accentuate the discontinuity of the field component across the interface thus placing a demanding test on the effectiveness of the interfacial treatments in the numerical algorithm.

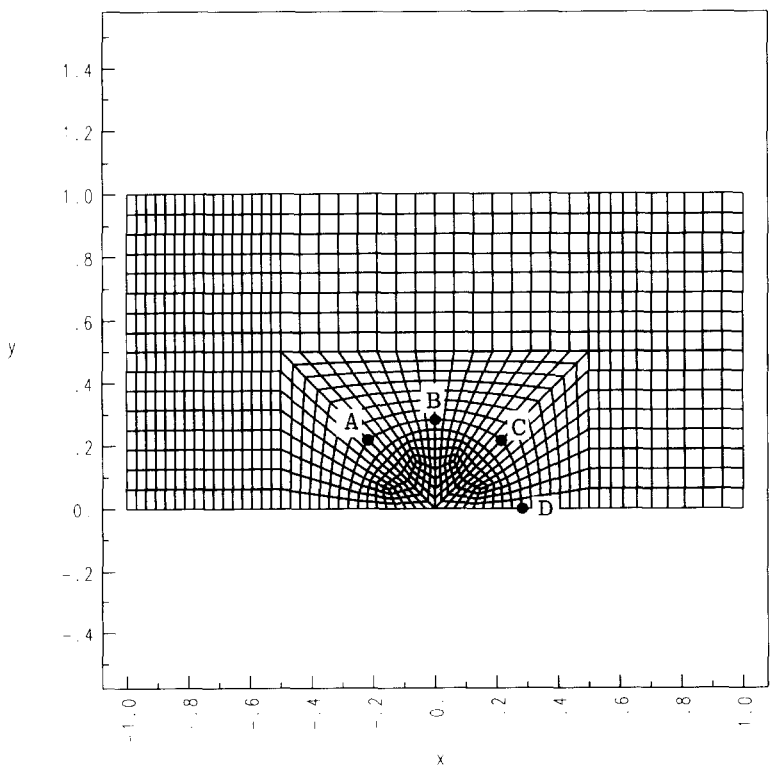

FIG. 4. The computational domain showing the material interface (at $r = 0.25$) with the locations of the observation points.

The temporal profile of the indicent wave, with time scaled in *ns*, is given by

$$E_t = \begin{cases} \frac{1}{2}\sqrt{\mu_0/\varepsilon_0}\{1-\cos 2\pi t\}; & 0 \leqslant t \leqslant 1, \\ 0; & t > 1. \end{cases}$$

Due to lack of an effective "free-space" (non-reflective) boundary condition, we have taken the simplest approach by assuming that the computational boundaries are perfect conductors ($E_n = 0$). We impose a symmetry condition of $E_x = 0$ along the centerline ($y = 0$). The time integration is carried out to a time of 8 *ns* at a constant timestep of 0.01 ns. The corresponding Courant number based on the properties of the cylinder is approximately 0.8.

The purpose of this numerical simulation is to compare the performances of two element approximations, namely, the lumped mass ELHL element in which the interface constraint (Eq. (16)) is specifically imposed, and, the ECHL element in which the material interface condition is incorporated naturally via the formulation. Figures 5 and 6 show the calculated time histories at nodes A ($r = 0.31$, $\theta = 3\pi/4$), B ($r = 0.28$, $\theta = \pi/2$), C ($r = 0.31$, $\theta = \pi/4$), and D ($r = 0.28$, $\theta = 0$) all of which are located in Fig. 4. The chosen nodes were in the neighborhood of the material interface in order to display minimal effect of reflections from computational boundaries, at least at early times. Furthermore, the nodes which are closest to the interface would be expected to be most sensitive to errors if interface conditions are improperly treated in the formulation.

The results show that the ECHL solution is noticebly more accurate that the ELHL solution in reproducing both the amplitude and shape of the exact waveform. Also, the amount of distortion of the wave caused by the computational boundaries appear to be substantially less significant for the ECHL formulation as shown by the magnitude of the trailing oscillations at late times. In both formulations the wiggles in the solutions are caused by a combined effect of wave scattering from interfaces which are associated with changes in mesh resolution and also by reflections from the external boundaries. We note that better agreement between the ECHL and the exact solution can be achieved if a finer mesh is employed and the computational boundaries are moved further away from the circular material interface. Figure 7 shows snapshots of the electric field at various times during the ECHL simulation. At an early time of 2 ns the plane wave approached the material interface from the left but did not yet interact with it. After 3 ns or so the waves have already penetrated into the material cylinder generating both transmitted and reflected waves at 4 ns. During this time the waves patterns become increasingly complex. Finally, at 6 ns, the incident wave has exited from the right boundary of the cylinder and the scattered waves began to interact with both the left and the right computational boundaries.

In order to assess the importance of the interface conditions, we performed a calculation with the ELHL element in which the interface was purposely ignored (i.e., Eq. (16) was not imposed at the interface nodes) and compared this with the ELHL solution generated with the full interface treatment. The E_y profiles (the vector

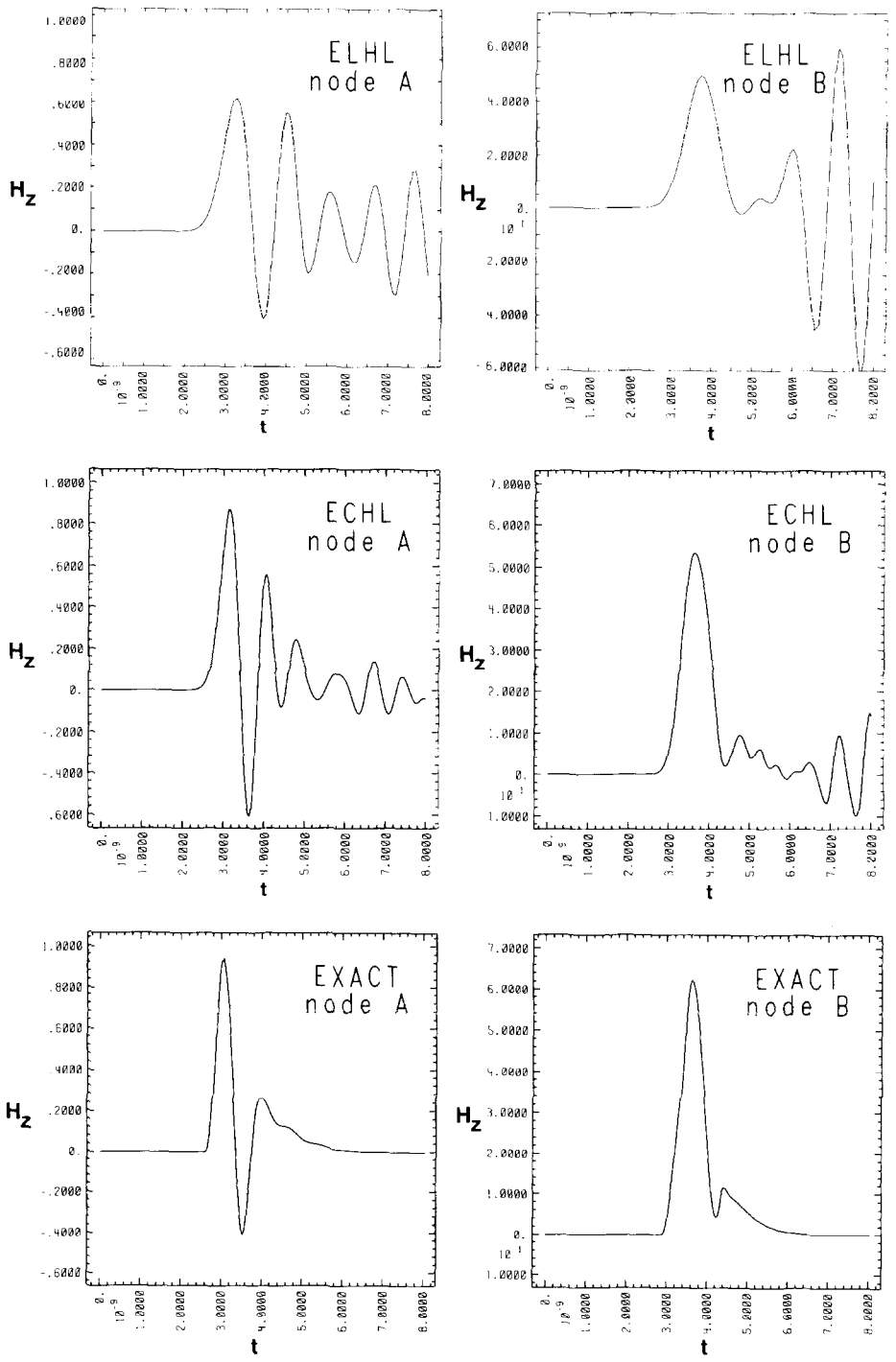

FIG. 5. Computed versus exact time history solutions for the circular material interface problem at the observation points A and B in Fig. 4. Numerical results are shown for the ELHL (top) and ECHL (center) formulations.

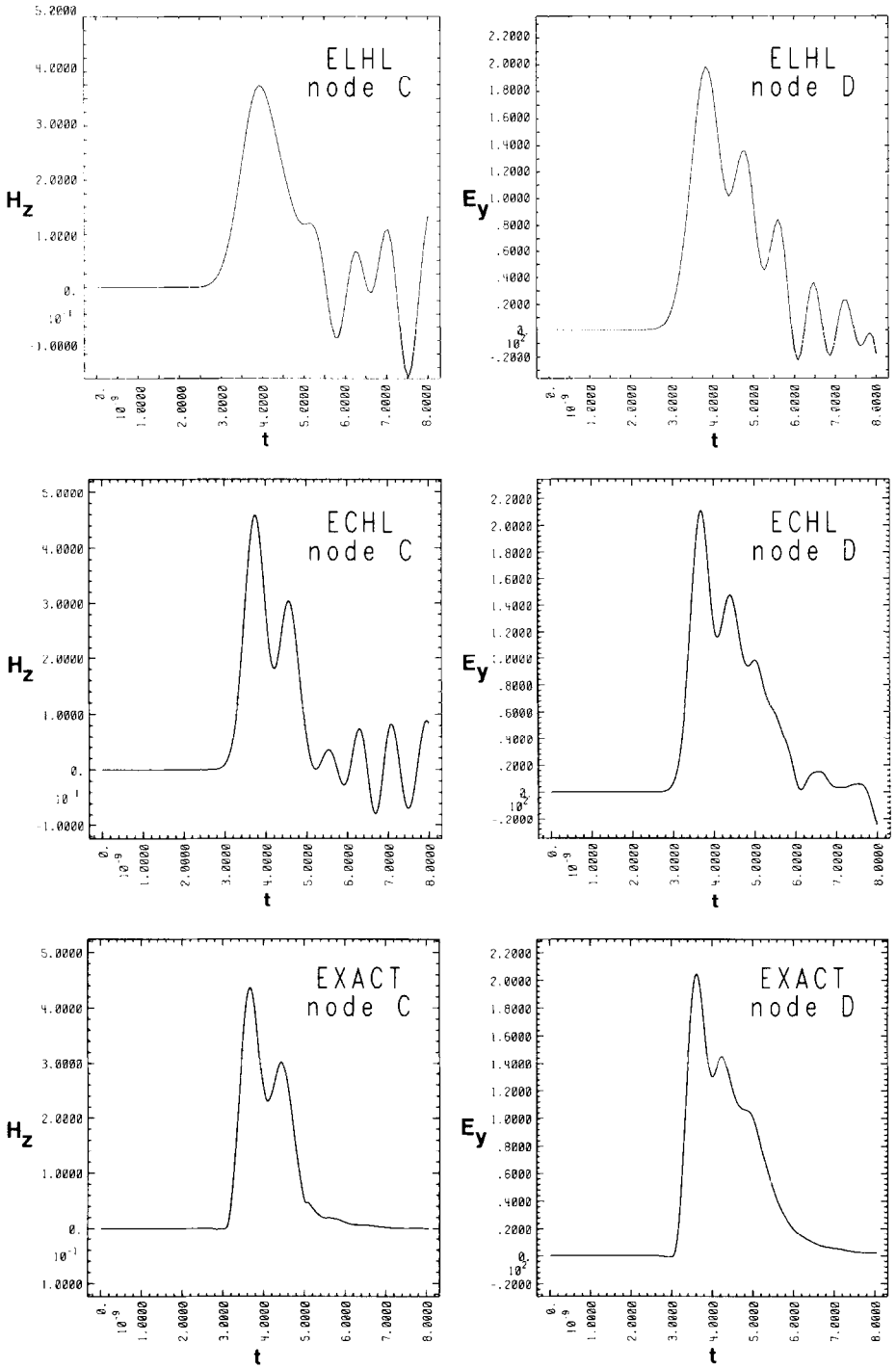

FIG. 6. Same as Fig. 5 except for the observation points C and D.

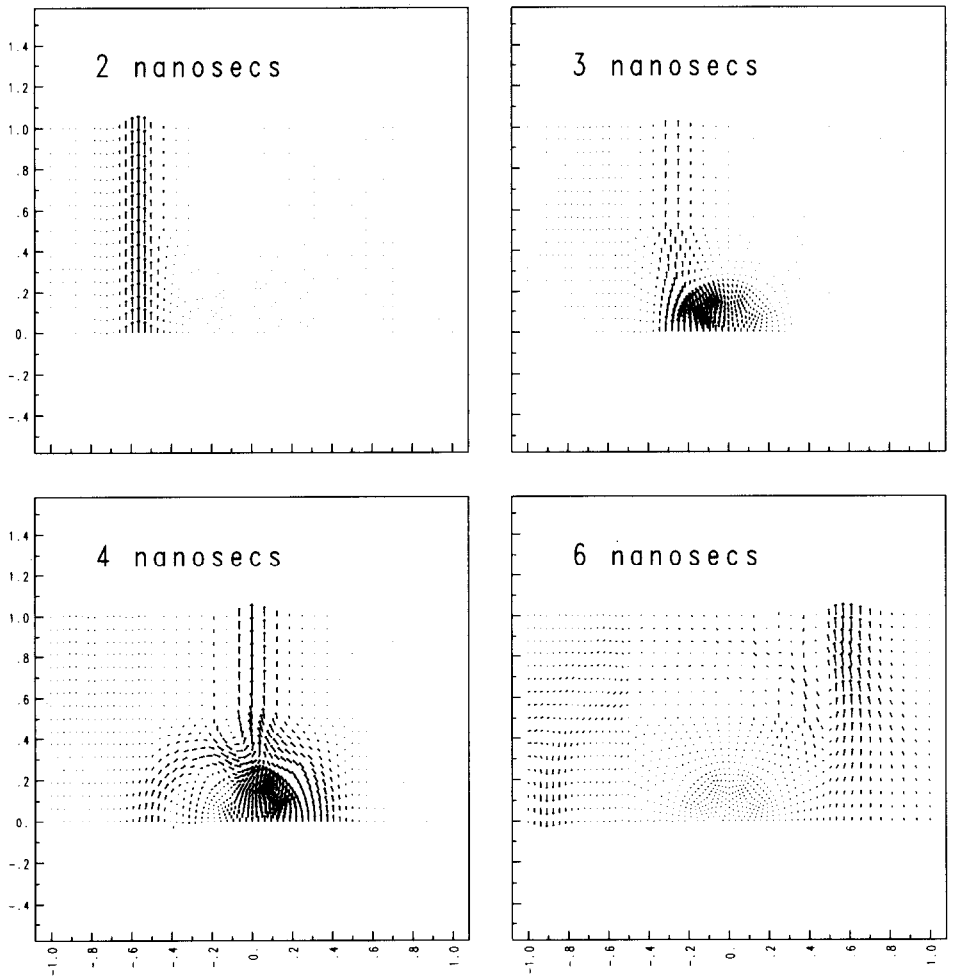

FIG. 7. Electric field vectors showing wave propagation through the circular material interface at various times.

component which is discontinuous across the interface) for the cross-section $x = 0$ at $t = 4.32$ ns is shown in Fig. 8. Except at the immediate vicinity of the interface, the two solutions agreed surprisingly well. It is interesting to note that the formulation which ignored the interface condition displayed a solution which approximately averaged the values between the closest nodes in the neighborhood of the interface. This result suggests, therefore, that if detailed description of the field at the interface is not of interest, it is probably not essential to impose specific interface constraints, at least for finite element formulations. In many instances the Galerkin procedure will, by construction, attempt to generate the best possible fit to the solution based on the given node distribution.

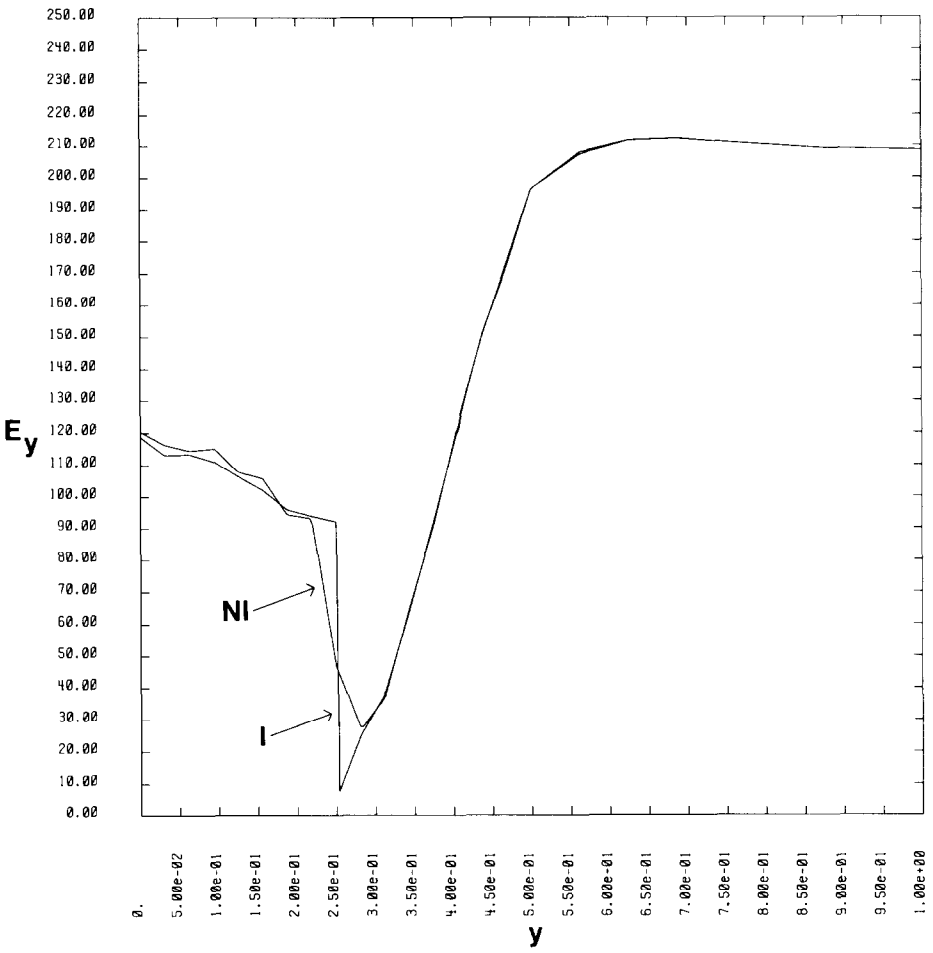

FIG. 8. The spatial variation of E_y along $x = 0$ at $t = 4.32$ ns showing the interfacial discontinuity at $y = 0.25$. "I" denotes the lumped mass ELHL solution with full interface treatment and "NI" denotes the same element but with no special interface treatment.

8. CONCLUSIONS

We have presented a new finite element solution technique for the Maxwell's equations which is based on a mixed formulation. The technique is computationally cost-effective and appears to exhibit, even on distorted meshes, the good accuracy of staggered-grid difference schemes. Moreover, an explicit time integration scheme can be easily implemented since the formulation simplies certain consistent mass matrices into diagonal forms. Of the mixed formulations discussed, the ECHL formulation is particularly advantageous for treatment of prescribed boundary

conditions and for calculations involving certain material interfaces. Finally it appears that the finite element procedure automatically generates an "averaged" solution across a material interface without the necessity of imposing special interface conditions.

ACKNOWLEDGMENTS

This paper is an extended version of a paper which appeared in the "Proceedings, of the First Woodward Conference on Wave Phenomena, Theoretical, Computational and Practical Aspects, June 2–3, 1988 at San Jose State University, San Jose." The authors acknowledge the assistance of Scott Ray of LLNL in providing a number of exact solutions of problems considered in this study. This work was performed under the auspices of the U.S. Department of Energy by the Lawrence Livermore National Laboratory under Contract No. W-7405-Eng-48.

REFERENCES

1. P. L. ARLETT, A. K. BAHRANI, AND O. C. ZIENKIEWICZ, *Proc. IEEE* **115**, 1762 (1968).
2. P. P. SILVESTER AND R. L. FERRARI, *Finite Elements for Electrical Engineers* (Cambridge Univ. Press, London, 1983), p. 180.
3. M. V. K. CHARI AND P. P. SILVESTER (Eds.), *Finite Elements in Electric and Magnetic Field Problems* (Wiley, Chichester, 1980), p. 219.
4. D. R. LYNCH, K. D. PAULSEN, AND J. W. STROHBEHN, *J. Comput. Phys.* **58**, 246 (1985).
5. A. C. CANGELLARIS, C. C. LIN, AND K. K. MEI, *IEEE Trans. Antennas Propag.* **AP 35**, 1160 (1967).
6. A. TAFLOVE, *IEEE Trans. Electromagn. Compat.* **EMC 22**, 191 (1980).
7. K. K. MEI, A. CANGELLARIS, AND D. J. ANGELAKOS, *Radio Sci.* **19**, 1145 (1984).
8. R. T. WILLIAMS AND O. C. ZIENKIEWICZ, *Int. J. Num. Methods Fluids* **1**, 81 (1981).
9. M. J. P. CULLEN, *J. Comput. Phys.* **51**, 291 (1983).
10. N. K. MADSEN AND R. W. ZIOLKOWSKI, *Wave Motion* **10**, 583 (1988).
11. O. C. ZIENKIEWICZ, *The Finite Element Method in Engineering Science*, 2nd ed. (McGraw–Hill, New York, 1971), p. 787.
12. A. MIZUKAMI, *Comput. Methods Appl. Mech. Eng.* **59**, 111 (1986).
13. F. MESINGER AND A. ARAKAWA, GARP Publ. Ser. 17, Vol. 1, WMO-ICSU, Geneva, 1976 (unpublished).
14. J. DONEA AND S. GUILIANI, *Int. J. Num. Methods Fluids* **1**, 63 (1981).
15. M. S. ENGELMAN, R. L. SANI, AND P. M. GRESHO, *Int. J. Num. Methods Fluids* **2**, 225 (1982).
16. R. L. LEE, P. M. GRESHO, AND R. L. SANI, *Int. J. Num. Methods Eng.* **14**, 1785 (1979).
17. R. F. HARRINGTON, *Time Harmonic Electromagnetic Fields* (McGraw–Hill, New York, 1961), p. 480.